

Doping effects on electronic states in electron-doped FeSe: Impact of self-energy and vertex corrections

Youichi Yamakawa, Seiichiro Onari, and Hiroshi Kontani
Department of Physics, Nagoya University, Nagoya 464-8602, Japan
 (Dated: January 26, 2022)

The pairing glue of high- T_c superconductivity in heavily electron-doped (e-doped) FeSe, in which hole-pockets are absent, has been an important unsolved problem. Here, we focus on a heavily e-doped bulk superconductor $\text{Li}_{1-x}\text{Fe}_x\text{OHFeSe}$ ($T_c \sim 40$ K). We construct a multiorbital model beyond the rigid band approximation and analyze the spin and orbital fluctuations by taking both vertex corrections (VCs) and self-energy into consideration. Without e-doping ($x = 0$), the ferro-orbital order without magnetism in FeSe is reproduced by the VCs. The orbital order quickly disappears when the hole-pocket vanishes at $x \sim 0.03$. With increasing x further, the spin fluctuations remain small, whereas orbital fluctuations gradually increase with x due to the VCs. The negative feedback due to the self-energy is crucial to explain experimental phase diagram. Thanks to both vertex and self-energy corrections, the orbital-fluctuation-mediated s_{++} -wave state appears for a wide doping range, consistent with experiments.

The high- T_c superconducting (SC) state in heavily electron-doped (e-doped) FeSe systems attracts great attention, but its pairing mechanism is still an open question. One of the characteristics of e-doped FeSe is the lack of magnetic order. Bulk FeSe exhibits spontaneous orbital polarization $n_{xz} \neq n_{yz}$ at $T_S = 90$ K, whereas no magnetic order occurs down to the SC transition temperature $T_c = 9$ K [1]. The SC state has been studied intensively [1–7]. On the other hand, the orbital order is suppressed by only a few-percent e-doping, and instead, a high- T_c SC phase with $T_c \geq 40$ K appears for a wide doping range in various e-doped FeSe compounds, such as an ultra-thin FeSe layer on SrTiO_3 ($T_c = 40\text{--}100$ K) [8–12], K-doped FeSe ($T_c \sim 40$ K) [13, 14], and intercalated superconductors ($T_c \sim 40$ K) [15–21]. Angle-resolved photoemission spectroscopy (ARPES) and scanning tunneling microscopy (STM) measurements have revealed that the SC gaps on the electron Fermi surfaces (FSs) are fully gapped [9–11, 17–21].

In usual Fe-based superconductors with electron-FSs (eFSs) and hole-FSs (hFSs), strong spin orbital fluctuations coexist in many compounds. This fact means that two kinds of s -wave SC states, the s_{\pm} -wave state with sign reversal and the s_{++} -wave state without sign reversal, can be mediated by spin and orbital fluctuations, respectively [22–28]. Up to now, much experimental effort has been devoted to detecting the presence or absence of sign reversal [2, 4, 29–32]. The recently reported impurity-induced $s_{\pm} \rightarrow s_{++}$ crossover in $\text{Ba}(\text{Fe,Rh})_2\text{As}_2$ [33, 34] has clarified the coexistence of sizable repulsive and attractive pairing glues in Fe-based compounds.

In e-doped FeSe compounds, in contrast, the top of the hFSs completely sinks below the Fermi level [9, 13, 19]. In spite of its high T_c , NMR studies have revealed that the spin fluctuations at T_c in e-doped FeSe are considerably weaker than those in undoped FeSe [35]. It is still a significant mystery that the high- T_c state ($T_c > 40$ K) is realized in e-doped FeSe in spite of its weak spin fluctuation. Therefore, the pairing glue for the high- T_c state in e-doped FeSe is still controversial. Up to now, d -wave

state [36–39] and incipient s_{\pm} -wave state [37, 40, 41] have been proposed based on the spin fluctuation theory, while T_c will not be high. In FeSe/ SrTiO_3 , it is expected that strong interfacial electron-phonon coupling increases T_c up to ~ 60 K [8, 9, 42, 43]. However, $T_c \sim 40$ K is realized in $(\text{Li,Fe})\text{OHFeSe}$ even in the absence of strong interfacial electron-phonon interaction [16], indicating that the main pairing glue originates from electron correlations.

The present authors investigated the pairing mechanism in e-doped FeSe by focusing on the vertex corrections (VCs) that induce the orbital order and fluctuations [44]. It was found that orbital-fluctuation-mediated s_{++} -wave SC can occur even in the absence of hFSs. This result is consistent with the recent quasiparticle interference (QPI) measurement reported in Ref. [10], while another QPI study indicates sign reversal between inner- and outer-electron FSs [17, 21]. However, the reason that a high- T_c state is realized in various e-doped FeSe families for a very wide doping range ($x = 0.05\text{--}0.20$) was not explained [12, 14]. Therefore, further progress on the theory of pairing mechanisms is still necessary.

In this paper, we discuss the mechanism of high- T_c superconductivity in bulk heavily e-doped compound $\text{Li}_{1-x}\text{Fe}_x\text{OHFeSe}$ ($T_c \sim 40$ K). To understand the x - T phase diagram with wide superconducting region, we analyze the model using the self-consistent-vertex correction (SC-VC) theory [44–46], by incorporating the x -dependent self-energy into the theory [47]. At $x = 0$, the ferro-orbital order without magnetism in FeSe is reproduced. With increasing x , the orbital order quickly disappears, and spin fluctuations remain small for $0.05 < x < 0.20$. Interestingly, orbital fluctuations start to increase gradually for $x > 0.06$. Therefore, the orbital-fluctuation-mediated s_{++} -wave state appears for a wide doping range, in agreement with experiments. The x -dependent self-energy is crucial to explain the appropriate e-doping phase diagrams of FeSe compounds.

The key ingredient of the present orbital/spin fluctuation theory is the interference process between spin- and orbital-fluctuations shown in Fig. 1(a) [48]. The

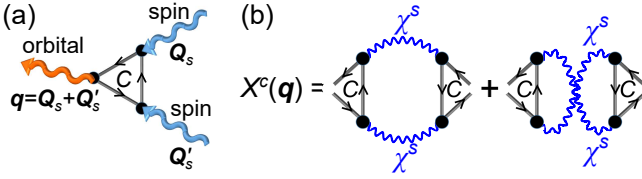


FIG. 1. (a) Interference process between spin- and orbital-fluctuations. C is the three-boson coupling made by electron Green functions. (b) Charge channel χ -VC X^c .

three-boson coupling C is given by three electron Green functions. The correction for the orbital susceptibility in Fig. 1(b), which we call the χ -VC, is composed of the process in Fig. 1(a) twice. Note that the χ -VC at $\mathbf{q} = \mathbf{0}$ is proportional to $\sum_{\mathbf{q}} \{\chi^s(\mathbf{q})\}^2 \propto \max_{\mathbf{q}} \chi^s(\mathbf{q})$ in two-dimensional systems [45, 49]. This “positive feedback” through χ -VC is the physical reason why orbital fluctuations are enlarged by spin fluctuations [45]. This bottom-up approach towards strongly correlated systems by introducing the VCs enables us to explain the nematicity and anomalous transport phenomena in Refs. [45, 50].

Here, we construct the model Hamiltonian for $\text{Li}_{1-x}\text{Fe}_x\text{OHFeSe}$. We first perform the WIEN2k band calculation for general x using the virtual crystal approximation (VCA). Next, we derive the eight-orbital tight-binding model \hat{H}_x^{VCA} using the Wannier90 package. Then, the unfolded eight-orbital d - p Hubbard model for $\text{Li}_{1-x}\text{Fe}_x\text{OHFeSe}$ is given as $\hat{H} = \hat{H}_x^0 + r\hat{H}^U$, where $\hat{H}_x^0 = \hat{H}_x^{\text{VCA}} + \hat{\Sigma}^{\text{exp}}(\mathbf{k})$. Here, the static self-energy $\hat{\Sigma}^{\text{exp}}(\mathbf{k})$ is introduced to reproduce the experimental FSs of FeSe at $x = 0$ [51–55], by following Ref. [46]. The microscopic derivation of $\hat{\Sigma}^{\text{exp}}(\mathbf{k})$ [56, 57] is an important future issue. \hat{H}^U is the first-principles screened Coulomb interaction for d orbitals in FeSe (averaged Coulomb interaction is 7.2 eV) [58], and r is the reduction factor. In the present study, we fix $r = 0.355$ to reproduce weakly developed spin fluctuations for $x = 0 \sim 0.2$ above T_S [59, 60]. More detailed explanation is summarized in the Supplemental Material (SM) A [61].

Figures 2(a) and (b) show the folded FSs in the two-Fe Brillouin zone (BZ) derived from \hat{H}_x for $x = 0$ and 0.15, respectively. Here, we introduced the spin-orbit interaction (SOI) $\eta_{\text{SOI}}\mathbf{l} \cdot \mathbf{s}$ with $\eta_{\text{SOI}} = 50$ meV. At $x = x_c \sim 0.03$, the hFS around the Γ point disappears. The d -orbital density of states (DOS) at the Fermi level is shown in Fig. 2(c). As x increases from $x = 0$, both the total DOS and xz orbital DOS decrease for $x \leq x_c$. For $x > x_c$, the xy -orbital DOS is dominant and it increases gradually with doping. The DOS in the FeSe rigid-band approximation ($\hat{H}_{x=0}^0$) is smaller than the DOS in the present VCA-based model, consistently with a previous study on K-doped FeSe [62]. This non-rigid-band increment of the DOS magnifies T_c for $x \sim 0.2$.

The self-energy in the fluctuation exchange (FLEX)

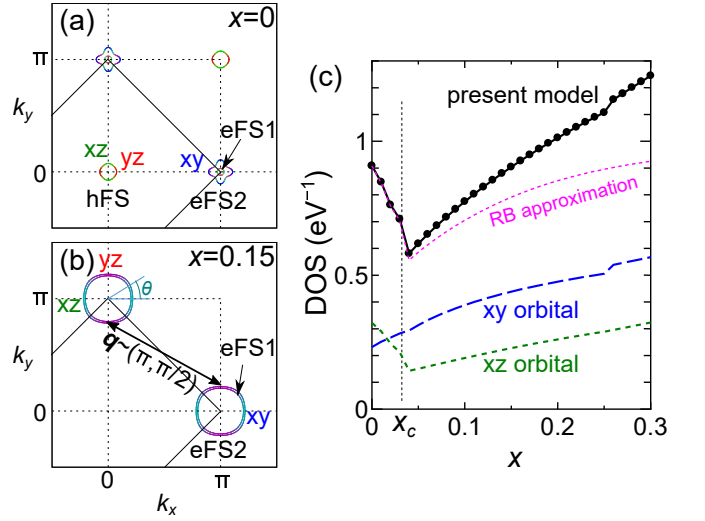


FIG. 2. (a)(b) FSs for (a) $x = 0$ and (b) 0.15 in the folded BZ with $\eta_{\text{SOI}} = 50$ meV. The green, red, and blue lines correspond to the xz , yz , and xy orbitals, respectively. eFS1 and eFS2 are inner and outer eFSs, respectively. $\mathbf{q} = (\pi, \pi/2)$ is the nesting vector; eFS1 touches eFS2 by the translational wavevector \mathbf{q} . (c) x dependence of d -orbital DOS at the Fermi level. The hFS around Γ disappears at $x_c \sim 0.03$.

approximation [63] in the absence of the SOI is given as

$$\Sigma_{l,m}(k) = \frac{T}{N} \sum_{k',l',m'} V_{l,l';m,m'}^\Sigma(k-k') G_{l',m'}(k'), \quad (1)$$

where $\hat{V}^\Sigma = \frac{3}{2}\hat{V}^s + \frac{1}{2}\hat{V}^c$, $k = (\mathbf{k}, \epsilon_n = \pi T(2n+1))$, and l, l', m, m' represent the d -orbital indices. ($l = 1, 2, 3, 4, 5$ corresponds to $3z^2 - r^2, xz, yz, xy, x^2 - y^2$ orbitals.) The electron Green function is $\hat{G}(k) = [\{\hat{G}^0(k)\}^{-1} - \hat{\Sigma}(k)]^{-1}$, where $\hat{G}^0(k)$ is the bare Green function.

The spin (charge) susceptibility is $\hat{\chi}^{s(c)} = \hat{\chi}^0 [\hat{1} - \hat{U}^{s(c)} \hat{\chi}^0]^{-1}$, where $\chi_{l,l';m,m'}^0(\mathbf{q}) = -\frac{T}{N} \sum_k G_{l,m}(k+\mathbf{q}) G_{m'l'}(k)$ is the irreducible susceptibility. The spin (charge) channel interaction in Eq. (1) is $\hat{V}^{s(c)} = \hat{U}^{s(c)} + \hat{U}^{s(c)} \hat{\chi}^{s(c)} \hat{U}^{s(c)}$, where $\hat{U}^{s(c)}$ is the spin (charge) channel Coulomb interaction. The self-energy represents the mass-enhancement and quasiparticle damping due to spin fluctuations. Here, to keep the shape of FSs, we drop the static Hermite part in the self-energy $(\hat{\Sigma}(\mathbf{k}, +i\delta) + \hat{\Sigma}(\mathbf{k}, -i\delta))/2$ [47, 64].

Figure 3(a) shows total spin susceptibility $\chi^s(\mathbf{q}) \equiv \sum_{l,m} \chi_{l,l';m,m}^s(\mathbf{q})$ for $x = 0$ and 0.2 with $r = 0.355$. Here, we calculate χ^s at low T ($=1$ meV) in order to clarify its peak structure. At $x = 0$, $\chi^s(\mathbf{q})$ has commensurate peaks at $\mathbf{q} = (\pi, 0)$ and $(0, \pi)$ due to the nesting between hFS and eFSs. In addition, broad peak appears around $\mathbf{q} = (\pi, \pi)$. At $x = 0.2$, $\chi^s(\mathbf{q})$ has incommensurate peaks at the nesting vector between eFSs shown in 2(b), which is observed experimentally [60]. The importance of the latter nesting has been stressed in various FeSe and FeAs compounds in literatures [22, 36, 37, 47].

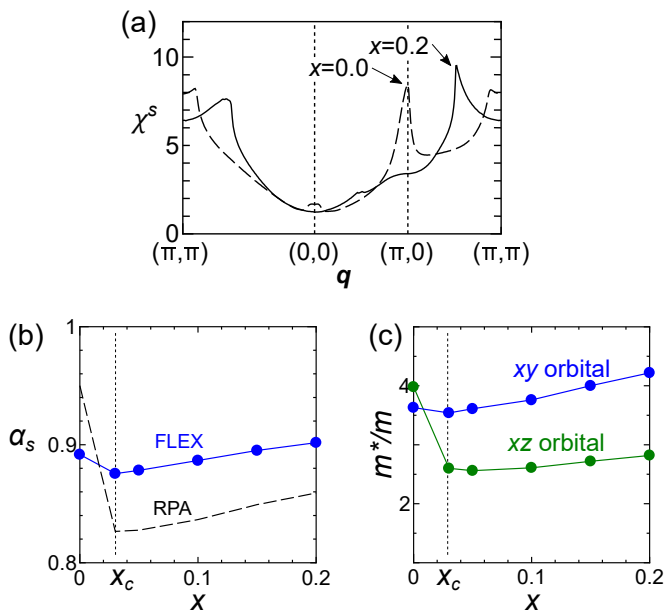


FIG. 3. (a–c) Total spin susceptibility $\chi^s(\mathbf{q})$ for (a) $x = 0$ and (b) $x = 0.2$ for $T = 1$ meV. (c) x dependence of spin Stoner factors α_s . (d) Mass-enhancement factors $Z = m^*/m$ for xz and xy orbitals. Here, $r = 0.355$ and 0.218 are used in the FLEX and RPA calculations, respectively.

Figure 3(b) shows the x dependence of the spin Stoner factor α_s , which is the maximum eigenvalues of $\hat{U}^s \hat{\chi}^0(\mathbf{q})$; ($\alpha_s = 1$ is the magnetic critical point.) The obtained spin fluctuations remains small even for heavily e-doped case, which is consistent with NMR results [35]. A similar result is also obtained by the random-phase approximation (RPA) for $r = 0.209$. Figure 3(c) shows the mass-enhancement factor $Z = m^*/m$ given by the self-energy for xz (yz) and xy orbitals. Z_{xy} is approximately 3–4 and is larger than Z_{xz} for $x > x_c$, due to the strong spin fluctuations and large DOS on the xy orbital. The obtained values agree with a previous dynamical mean-field theory (DMFT) studies [62, 65].

Next, we study the orbital susceptibility by including the VC for the susceptibility χ -VC (\hat{X}^c) and Σ [47]. Here, we consider the Aslamazov-Larkin (AL) processes shown in Fig. 1(b) and analytically shown in SM B [61], because its significance in Fe-based superconductors has been discovered in previous studies [5, 44–47, 49]. At $x = 0$, strong orbital fluctuations with respect to $O \equiv n_{xz} - n_{yz}$ appears due to the AL term [45, 46]. In this case, $\chi_{l,m}^c(\mathbf{q}) \equiv \chi_{l,l;m,m}^c(\mathbf{q})$ shows large positive (negative) value for $l = m = 2$ and 3 ($l = 2, m = 3$) at $\mathbf{q} = \mathbf{0}$, and they diverge when orbital order $n_{xz} \neq n_{yx}$ appears.

Hereafter, we set $T = 20$ meV. Figure 4(a) shows the numerical results for $x = 0$. Due to the χ -VC on xz, yz orbitals, $\chi_{2;2}^c(\mathbf{0})$ develops divergently due to the χ -VC in spite of the weak spin fluctuations in FeSe [46]. Since $\chi_{2;3}^c(\mathbf{0}) \approx -\chi_{2;2}^c(\mathbf{0})$, strong ferro-orbital fluctuations with respect to $O_{x^2-y^2} \equiv n_{xz} - n_{yz}$ in undoped FeSe is sat-

isfactorily explained. The non-magnetic nematic order can be explained in the present theory as discussed in Ref. [46] and SM C [61]. In contrast, $\chi_{4;4}^c$ ($4 = xy$ orbital) remains small because the χ -VC on xy orbital is unimportant due to the smallness of xy orbital spin fluctuations.

In contrast, for $x = 0.2$, strong ferro-orbital fluctuations with respect to $O_{z^2} \equiv n_{xy} - (n_{xz} + n_{yz})/2$ appears. The obtained $\chi_{4;4}^c(\mathbf{q})$ is shown in Fig. 4(b), and the relations $\chi_{2;2}^c \approx \chi_{4;4}^c/4$, $\chi_{2;4}^c \approx -\chi_{4;4}^c/2$ and $\chi_{2;3}^c \approx \chi_{4;4}^c/4$ holds. As we discussed in Ref. [47], O_{z^2} orbital fluctuations develop when the χ -VC develop for all $2 \sim 4$ orbitals. The crossover of dominant orbital fluctuations from $O_{x^2-y^2}$ to O_{z^2} occurs at $x \sim x_c$, reflecting the increment of xy -orbital spin fluctuations due to inter-eFS nesting. Both $O_{x^2-y^2}$ - and O_{z^2} -orbital fluctuations at $\mathbf{q} \sim \mathbf{0}$ enlarge T_c irrespective of the gap symmetry [25, 66].

Figure 4(c) shows the x -dependence of the charge Stoner factor α_c , which is the maximum eigenvalue of $\hat{U}^c(\hat{\chi}^0 + \hat{X}^c)$. Thus, α_c is strongly enlarged by the χ -VC. Here, $\alpha_c \sim 1$ for $x = 0$ corresponds to the ferro-orbital order ($n_{xz} \neq n_{yz}$) in undoped FeSe. Through doping, α_c drops quickly since hFS disappears at $x = x_c$. Interestingly, α_c gradually increases for $x \gtrsim x_c$, indicating the orbital-fluctuation-mediated superconductivity in the absence of the hFS.

To confirm the numerical results in Fig. 4, we also analyze the same model based on the density-wave (DW) equation developed in Ref. [67–70] in SM D [61]. By solving the DW equation, the higher-order AL processes are automatically generated. Also, the criteria of the conserving approximation [71] are satisfied by including the FLEX self-energy. At $x = 0$ and $x = 0.25$, strong ferro-orbital fluctuations are obtained, consistently with Figs. 4(a) and 4(b). In addition, strong incommensurate charge channel fluctuations at $\mathbf{q} \approx (\pi, \pi/2)$ develop at $x = 0.25$. They are overlooked in the SC-VC theory since the strong \mathbf{k} -dependence of the form factor, which represents the fluctuation of hopping integrals, is essential. This incommensurate “bond fluctuations” will be important for the pairing mechanism in heavily e-doped FeSe.

Next, we study the SC state in e-doped FeSe by following the theoretical procedure reported in Refs. [44, 72]. The linearized gap equation is given by

$$\lambda_{SC} Z_\alpha(\mathbf{k}, \epsilon_n) \Delta_\alpha(\mathbf{k}, \epsilon_n) = -\frac{\pi T}{(2\pi)^2} \sum_{m,\beta} \oint_{\beta} \frac{d\mathbf{p}}{v_\beta(\mathbf{p})} V_{\alpha,\beta}^{SC}(\mathbf{k}, \epsilon_n; \mathbf{p}, \epsilon_m) \frac{\Delta_\beta(\mathbf{p}, \epsilon_m)}{|\epsilon_m|} \quad (2)$$

where λ_{SC} is the eigenvalue, which is roughly proportional to T_c , and the relation $\lambda_{SC} = 1$ is satisfied at $T = T_c$. Further, $\Delta_\alpha(\mathbf{k})$ is the gap function, $v_\alpha(\mathbf{k}) \equiv \frac{\partial \epsilon_\alpha(\mathbf{k})}{\partial \mathbf{k}}$ is the Fermi velocity, and $Z_\alpha(\mathbf{k})$ is the mass-enhancement factor. Here, α and β are the indices of the folded FSs with the SOI shown in Figs. 1(a) and (b), considering the significance of the SOI on the SC gap. We omit the SOI in calculating the pairing interaction since its influence

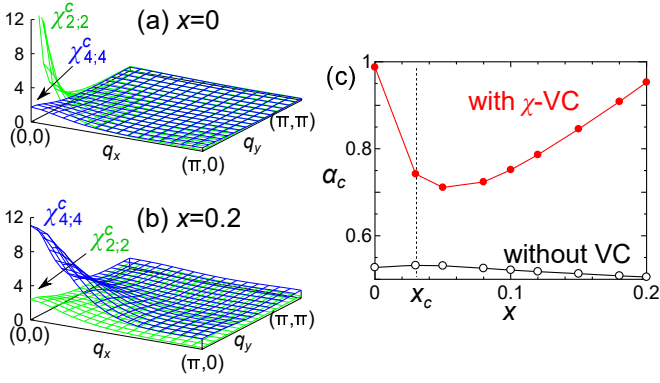


FIG. 4. (a) Orbital susceptibilities $\chi_{i;l}^c(\mathbf{q})$ for $l = 2 = xz$ (green) and $l = 4 = xy$ (blue) for $x = 0$. (b) $\chi_{i;l}^c(\mathbf{q})$ for $x = 0.2$. (c) x dependence of α_c with and without χ -VC. Here, we set $r = 0.355$.

on the fluctuations is small [72].

The pairing interaction V^{SC} in the present beyond the Migdal-Eliashberg (ME) formalism is shown in Fig. 5(a). The first term is the single-fluctuation exchange process with the VC for the electron-boson coupling, which we call the U -VC. The U -VC Λ^ν ($\nu = s, c$) is composed of the AL processes and Maki-Thompson (MT) term expressed in Fig. 5(b). The first term is symbolically expressed as $\hat{V}_\Lambda^{\text{SC}} = \sum_{\nu}^{s,c} b_\nu \hat{\Lambda}^\mu \hat{V}^\nu \hat{\Lambda}^\nu$, where $b_s = 3/2$ and $b_c = -1/2$. In the presence of moderate spin fluctuations, $|\Lambda^c|^2 \gg 1$ for low energy region near the Fermi momentum [73–75]. Therefore, U -VC is significant for the pairing mechanism.

The second crossing term $\hat{V}_{\text{cross}}^{\text{SC}}$ in Fig. 5(a) is one of the lowest beyond-ME processes that are absent in the first term. In Ref. [44], we revealed that $\hat{V}_{\text{cross}}^{\text{SC}}$ gives large attractive interaction between eFS1 and eFS2. The existence of this inter-pocket attractive pairing in heavily e-doped FeSe is confirmed based on the DW equation study as we explain in SM E [61]. It is found that $\hat{V}_{\text{cross}}^{\text{SC}}$ represents the inter-pocket attractive interaction due to the “bond fluctuations”.

Figure 5(c) shows the doping dependence of λ_{SC} . The fully gapped s_{++} -wave state has the largest eigenvalue throughout the entire doping region. The resulting λ_{SC} for the s_{++} -wave state is enhanced due to the synergy between U -VC and $V_{\text{cross}}^{\text{SC}}$, as we discuss in Ref. [44] in detail. The resulting fully gapped state with moderate anisotropy is shown in Fig. 5(d), which is consistent with experimental reports in Refs. [9–11, 19]. The relation with the SC state in bulk FeSe is briefly discussed in SM F [61]. In contrast, λ_{SC} for the spin-fluctuation-mediated d -wave state is small, since the spin fluctuations are weak and the gap is suppressed by the SOI-induced band mixing [42]. Note that fully-gapped d -wave state is realized if $\Delta \gtrsim \eta_{\text{SOI}}$ [39].

To clarify why the s_{++} -wave state is realized, we show in Fig. 5(e) the x dependence of the averaged intra- and inter-pocket interactions: $V_{\alpha,\beta}^{\text{ave}} \equiv \frac{1}{(2\pi)^2} \sum_{\epsilon_n, \epsilon_m = \pm\pi T} \oint_\alpha \frac{d\mathbf{k}}{v_\alpha(\mathbf{k})} \oint_\beta \frac{d\mathbf{p}}{v_\beta(\mathbf{p})} V_{\alpha,\beta}^{\text{SC}}(\mathbf{k}, \epsilon_n; \mathbf{p}, \epsilon_m)$.

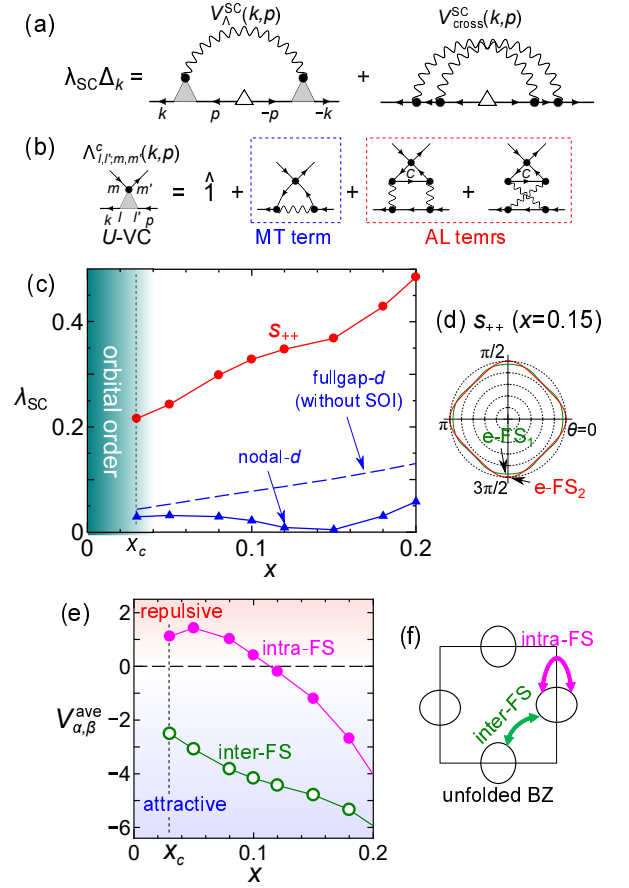


FIG. 5. (a) Beyond-ME gap equation in the present analysis. Both the first term V_Λ^{SC} and the second term $V_{\text{cross}}^{\text{SC}}$ are significant. (b) Charge channel U -VC Λ^c . (c) x dependence of eigenvalues of linearized gap equation λ_{SC} . Here, the SOI $\eta_{\text{SOI}} = 50$ meV is considered except for the dashed lines. $x < x_c$ is the orbital order region. (d) Angle θ dependence of s_{++} -wave gap function on FSs for $x = 0.15$. (e) Averaged intra-FS ($\alpha = \beta$) and inter-FS ($\alpha \neq \beta$) interactions $V_{\alpha,\beta}^{\text{ave}}$ on FSs in (f) unfolded BZ without SOI.

Here, we consider two electron-pockets in unfolded BZ without the SOI shown in Fig. 5(f). The intra-FS ($\alpha = \beta$) interaction changes from positive to negative with e-doping because of the development of the orbital fluctuations shown in Fig. 4(c). In addition, sizable attractive inter-FS ($\alpha \neq \beta$) interaction is mainly given by $V_{\text{cross}}^{\text{SC}}$, as we discussed in Ref. [44] and in SM E [61].

It is interesting to discuss the similarities between e-doped FeSe and heavily e-doped $Re\text{FeAsO}$ ($Re = \text{rare earth}$), both of which exhibit high- T_c phases in spite of weak spin fluctuations [35, 76]. These high- T_c compounds have very similar FSs: large eFSs and tiny or absent hFSs; The FSs in heavily e-doped $Re\text{FeAsO}$ are shown in Fig. 1(c) in Ref. [47]. As discussed in Ref. [47], the xy -orbital DOS is dominant, and weak spin fluctuations on the xy -orbital efficiently induce strong orbital fluctuations on the xy -orbital, χ_{xy}^c , due to the AL-VCs. The present analysis indicates that similar pairing mech-

anism is realized in these compounds.

The improvement of the self-energy beyond the FLEX approximation is one of the important future issues. We note that the enhancement of s -wave T_c in the Hund's metal state was discussed by a recent DMFT study [77].

In summary, we discussed the pairing mechanism in the heavily e -doped bulk compound $\text{Li}_{1-x}\text{Fe}_x\text{OHFeSe}$. At $x = 0$, the ferro-orbital order without magnetism in FeSe is reproduced. With increasing x , the orbital order quickly disappears, and the spin fluctuations remain weak for $0 < x < 0.20$. Interestingly, small spin fluctuations cause large orbital fluctuations due to the AL-VC X^{AL} for a wide doping range. Therefore, the

orbital-fluctuation-mediated s_{++} -wave state appears for $0.05 < x < 0.2$, consistent with experiments. Therefore, the orbital fluctuations will be the main pairing glue in both e -doped FeSe and H-doped 1111 systems.

ACKNOWLEDGMENTS

We are grateful to Y. Nomura for fruitful discussion on the doping effect on the band structure in FeSe beyond the rigid-band approximation. This work was supported by the Grants-in-Aid for Scientific Research from MEXT, Japan (No. JP19H05825, JP18H01175, JP17K05543, JP17K14338).

-
- [1] A. E. Böhmer and A. Kreisel, *J. Phys.: Condens. Matter* **30**, 023001 (2017).
- [2] Q. Wang, Y. Shen, B. Pan, Y. Hao, M. Ma, F. Zhou, P. Steffens, K. Schmalzl, T. R. Forrest, M. Abdel-Hafiez, X. Chen, D. A. Chareev, A. N. Vasiliev, P. Bourges, Y. Sidis, H. Cao, and J. Zhao, *Nat. Mater.* **15**, 159 (2016).
- [3] P. O. Sprau, A. Kostin, A. Kreisel, A. E. Böhmer, V. Taufour, P. C. Canfield, S. Mukherjee, P. J. Hirschfeld, B. M. Andersen, and J. C. S. Davis, *Science* **357**, 75 (2017).
- [4] Y. Sun, A. Park, S. Pyon, T. Tamegai, and H. Kitamura, *Phys. Rev. B* **96**, 140505(R) (2017).
- [5] Y. Yamakawa and H. Kontani, *Phys. Rev. B* **96**, 144509 (2017).
- [6] A. Kreisel, B. M. Andersen, P. O. Sprau, A. Kostin, J. C. S. Davis, and P. J. Hirschfeld, *Phys. Rev. B* **95**, 174504 (2017).
- [7] S.-H. Baek, J. M. Ok, J. S. Kim, S. Aswartham, I. Morozov, D. Chareev, T. Urata, K. Tanigaki, Y. Tanabe, B. Büchner, and D. V. Efremov, *npj Quantum Mater.* **5**, 8 (2020).
- [8] Q.-Y. Wang, Z. Li, W.-H. Zhang, Z.-C. Zhang, J.-S. Zhang, W. Li, H. Ding, Y.-B. Ou, P. Deng, K. Chang, J. Wen, C.-L. Song, K. He, J.-F. Jia, S.-H. Ji, Y. Wang, L. Wang, X. Chen, X. Ma, and Q.-K. Xue, *Chin. Phys. Lett.* **29**, 037402 (2012).
- [9] J. J. Lee, F. T. Schmitt, R. G. Moore, S. Johnston, Y.-T. Cui, W. Li, M. Yi, Z. K. Liu, M. Hashimoto, Y. Zhang, D. H. Lu, T. P. Devereaux, D.-H. Lee, and Z.-X. Shen, *Nature* **515**, 245 (2014).
- [10] Q. Fan, W. H. Zhang, X. Liu, Y. J. Yan, M. Q. Ren, R. Peng, H. C. Xu, B. P. Xie, J. P. Hu, T. Zhang, and D. L. Feng, *Nat. Phys.* **11**, 946 (2015).
- [11] Y. Zhang, J. J. Lee, R. G. Moore, W. Li, M. Yi, M. Hashimoto, D. H. Lu, T. P. Devereaux, D.-H. Lee, and Z.-X. Shen, *Phys. Rev. Lett.* **117**, 117001 (2016).
- [12] X. Shi, Z.-Q. Han, X.-L. Peng, P. Richard, T. Qian, X.-X. Wu, M.-W. Qiu, S. C. Wang, J. P. Hu, Y.-J. Sun, and H. Ding, *Nat. Commun.* **8**, 14988 (2017).
- [13] Y. Miyata, K. Nakayama, K. Sugawara, T. Sato, and T. Takahashi, *Nat. Mater.* **14**, 775 (2015).
- [14] C. H. P. Wen, H. C. Xu, C. Chen, Z. C. Huang, X. Lou, Y. J. Pu, Q. Song, B. P. Xie, M. Abdel-Hafiez, D. A. Chareev, A. N. Vasiliev, R. Peng, and D. L. Feng, *Nat. Commun.* **7**, 10840 (2016).
- [15] T. Noji, T. Hatakeda, S. Hosono, T. Kawamata, M. Kato, and Y. Koike, *Physica C* **504**, 8 (2014).
- [16] X. F. Lu, N. Z. Wang, H. Wu, Y. P. Wu, D. Zhao, X. Z. Zeng, X. G. Luo, T. Wu, W. Bao, G. H. Zhang, F. Q. Huang, Q. Z. Huang, and X. H. Chen, *Nat. Mater.* **14**, 325 (2015).
- [17] Z. Du, X. Yang, H. Lin, D. Fang, G. Du, J. Xing, H. Yang, X. Zhu, and H.-H. Wen, *Nat. Commun.* **7**, 10565 (2016).
- [18] Y. J. Yan, W. H. Zhang, M. Q. Ren, X. Liu, X. F. Lu, N. Z. Wang, X. H. Niu, Q. Fan, J. Miao, R. Tao, B. P. Xie, X. H. Chen, T. Zhang, and D. L. Feng, *Phys. Rev. B* **94**, 134502 (2016).
- [19] X. H. Niu, R. Peng, H. C. Xu, Y. J. Yan, J. Jiang, D. F. Xu, T. L. Yu, Q. Song, Z. C. Huang, Y. X. Wang, B. P. Xie, X. F. Lu, N. Z. Wang, X. H. Chen, Z. Sun, and D. L. Feng, *Phys. Rev. B* **92**, 060504(R) (2015).
- [20] M. Ren, Y. Yan, X. Niu, R. Tao, D. Hu, R. Peng, B. Xie, J. Zhao, T. Zhang, and D.-L. Feng, *Sci. Adv.* **3**, e1603238 (2017).
- [21] Q. Gu, Q. Tang, S. Wan, Z. Du, X. Yang, H. Yang, Q.-H. Wang, H. Lin, X. Zhu, and H.-H. Wen, *Phys. Rev. B* **98**, 134503 (2018).
- [22] K. Kuroki, S. Onari, R. Arita, H. Usui, Y. Tanaka, H. Kontani, and H. Aoki, *Phys. Rev. Lett.* **101**, 087004 (2008).
- [23] I. I. Mazin, D. J. Singh, M. D. Johannes, and M. H. Du, *Phys. Rev. Lett.* **101**, 057003 (2008).
- [24] S. Graser, G. R. Boyd, C. Cao, H.-P. Cheng, P. J. Hirschfeld, and D. J. Scalapino, *Phys. Rev. B* **77**, 180514(R) (2008).
- [25] H. Kontani and S. Onari, *Phys. Rev. Lett.* **104**, 157001 (2010).
- [26] A. V. Chubukov, D. V. Efremov, and I. Eremin, *Phys. Rev. B* **78**, 134512 (2008).
- [27] P. J. Hirschfeld, M. M. Korshunov, and I. I. Mazin, *Rep. Prog. Phys.* **74**, 124508 (2011).
- [28] Z. P. Yin, K. Haule, and G. Kotliar, *Nat. Phys.* **10**, 845 (2014).
- [29] M. Sato, Y. Kobayashi, S. Chul Lee, H. Takahashi, E. Satomi, and Y. Miura, *J. Phys. Soc. Jpn.* **79**, 014710 (2010); S. C. Lee, E. Satomi, Y. Kobayashi, and M. Sato, *ibid.* **79**, 023702 (2010).

- [30] J. Li, Y. F. Guo, S. B. Zhang, J. Yuan, Y. Tsujimoto, X. Wang, C. I. Sathish, Y. Sun, S. Yu, W. Yi, K. Yamaura, E. Takayama-Muromachiu, Y. Shirako, M. Akaogi, and H. Kontani, *Phys. Rev. B* **85**, 214509 (2012).
- [31] D. S. Inosov, J. T. Park, P. Bourges, D. L. Sun, Y. Sidis, A. Schneidewind, K. Hradil, D. Haug, C. T. Lin, B. Keimer, and V. Hinkov, *Nature Phys* **6**, 178 (2010).
- [32] C. Zhang, H.-F. Li, Y. Song, Y. Su, G. Tan, T. Netherton, C. Redding, S. V. Carr, O. Sobolev, A. Schneidewind, E. Faulhaber, L. W. Harriger, S. Li, X. Lu, D.-X. Yao, T. Das, A. V. Balatsky, Th. Brückel, J. W. Lynn, and P. Dai, *Phys. Rev. B* **88**, 064504 (2013).
- [33] G. Ghigo, D. Torsello, G. A. Ummarino, L. Gozzelino, M. A. Tanatar, R. Prozorov, and P. C. Canfield, *Phys. Rev. Lett.* **121**, 107001 (2018).
- [34] M. B. Schilling, A. Baumgartner, B. Gorshunov, E. S. Zhukova, V. A. Dravin, K. V. Mitsen, D. V. Efremov, O. V. Dolgov, K. Iida, M. Dressel, and S. Zapf, *Phys. Rev. B* **93**, 174515 (2016).
- [35] M. M. Hrovat, P. Jeglič, M. Klanjšek, T. Hatakeda, T. Noji, Y. Tanabe, T. Urata, K. K. Huynh, Y. Koike, K. Tanigaki, and D. Arçon, *Phys. Rev. B* **92**, 094513 (2015).
- [36] T. A. Maier, S. Graser, P. J. Hirschfeld, and D. J. Scalapino, *Phys. Rev. B* **83**, 100515(R) (2011).
- [37] T. Saito, S. Onari, and H. Kontani, *Phys. Rev. B* **83**, 140512(R) (2011).
- [38] Z.-X. Li, F. Wang, H. Yao, and D.-H. Lee, *Sci. Bull.* **61**, 925 (2016).
- [39] D. F. Agterberg, T. Shishidou, J. O'Halloran, P. M. R. Brydon, and M. Weinert, *Phys. Rev. Lett.* **119**, 267001 (2017).
- [40] X. Chen, S. Maiti, A. Linscheid, and P. J. Hirschfeld, *Phys. Rev. B* **92**, 224514 (2015).
- [41] V. Mishra, D. J. Scalapino, and T. A. Maier, *Sci. Rep.* **6**, 32078 (2016).
- [42] D.-H. Lee, *Chin. Phys. B* **24**, 117405 (2015).
- [43] L. Rademaker, Y. Wang, T. Berlijn, and S. Johnston, *New J. Phys.* **18**, 022001 (2016).
- [44] Y. Yamakawa and H. Kontani, *Phys. Rev. B* **96**, 045130 (2017).
- [45] S. Onari and H. Kontani, *Phys. Rev. Lett.* **109**, 137001 (2012).
- [46] Y. Yamakawa, S. Onari, and H. Kontani, *Phys. Rev. X* **6**, 021032 (2016).
- [47] S. Onari, Y. Yamakawa, and H. Kontani, *Phys. Rev. Lett.* **112**, 187001 (2014).
- [48] R. Tazai and H. Kontani, *Phys. Rev. B* **100**, 241103(R) (2019).
- [49] H. Kontani and Y. Yamakawa, *Phys. Rev. Lett.* **113**, 047001 (2014).
- [50] H. Kontani, *Rep. Prog. Phys.* **71**, 026501 (2008).
- [51] J. Maletz, V. B. Zabolotnyy, D. V. Evtushinsky, S. Thirupathiah, A. U. B. Wolter, L. Harnagea, A. N. Yaresko, A. N. Vasiliev, D. A. Chareev, A. E. Böhmer, F. Hardy, T. Wolf, C. Meingast, E. D. L. Rienks, B. Büchner, and S. V. Borisenko, *Phys. Rev. B* **89**, 220506(R) (2014).
- [52] K. Nakayama, Y. Miyata, G. N. Phan, T. Sato, Y. Tanabe, T. Urata, K. Tanigaki, and T. Takahashi, *Phys. Rev. Lett.* **113**, 237001 (2014).
- [53] T. Shimojima, Y. Suzuki, T. Sonobe, A. Nakamura, M. Sakano, J. Omachi, K. Yoshioka, M. Kuwata-Gonokami, K. Ono, H. Kumigashira, A. E. Böhmer, F. Hardy, T. Wolf, C. Meingast, H. v. Löhneysen, H. Ikeda, and K. Ishizaka, *Phys. Rev. B* **90**, 121111(R) (2014).
- [54] Y. Suzuki, T. Shimojima, T. Sonobe, A. Nakamura, M. Sakano, H. Tsuji, J. Omachi, K. Yoshioka, M. Kuwata-Gonokami, T. Watashige, R. Kobayashi, S. Kasahara, T. Shibauchi, Y. Matsuda, Y. Yamakawa, H. Kontani, and K. Ishizaka, *Phys. Rev. B* **92**, 205117 (2015).
- [55] T. Terashima, N. Kikugawa, A. Kiswandhi, E.-S. Choi, J. S. Brooks, S. Kasahara, T. Watashige, H. Ikeda, T. Shibauchi, Y. Matsuda, T. Wolf, A. E. Böhmer, F. Hardy, C. Meingast, H. v. Löhneysen, M.-T. Suzuki, R. Arita, and S. Uji, *Phys. Rev. B* **90**, 144517 (2014).
- [56] M. Hirayama, T. Miyake, and M. Imada *Phys. Rev. B* **87**, 195144 (2013).
- [57] J. M. Tomczak, M. van Schilfhaarde, and G. Kotliar *Phys. Rev. Lett.* **109**, 237010 (2012).
- [58] T. Miyake, K. Nakamura, R. Arita, and M. Imada, *J. Phys. Soc. Jpn.* **79**, 044705 (2010).
- [59] Q. Wang, Y. Shen, B. Pan, X. Zhang, K. Ikeuchi, K. Iida, A. D. Christianson, H. C. Walker, D. T. Adroja, M. Abdel-Hafez, X. Chen, D. A. Chareev, A. N. Vasiliev, and J. Zhao, *Nat. Commun.* **7**, 12182 (2016).
- [60] B. Pan, Y. Shen, D. Hu, Y. Feng, J. T. Park, A. D. Christianson, Q. Wang, Y. Hao, H. Wo, Z. Yin, T. A. Maier, and J. Zhao, *Nat. Commun.* **8**, 123 (2017).
- [61] See Supplemental Material.
- [62] Y. W. Choi and H. J. Choi, *Phys. Rev. Lett.* **122**, 046401 (2019).
- [63] N. E. Bickers and S. R. White, *Phys. Rev. B* **43**, 8044 (1991).
- [64] H. Ikeda, R. Arita, and Jan Kuneš *Phys. Rev. B* **81**, 054502 (2010).
- [65] Z. P. Yin, K. Haule, and G. Kotliar, *Nat. Mater.* **10**, 932 (2011).
- [66] J. Kang and R. M. Fernandes, *Phys. Rev. Lett.* **117**, 217003 (2016).
- [67] S. Onari, Y. Yamakawa, and H. Kontani, *Phys. Rev. Lett.* **116**, 227001 (2016).
- [68] S. Onari and H. Kontani, *Phys. Rev. B* **100**, 020507(R) (2019).
- [69] S. Onari and H. Kontani, *Phys. Rev. Research* **2**, 042005 (2020).
- [70] K. Kawaguchi, M. Tsuchiizu, Y. Yamakawa, and H. Kontani, *J. Phys. Soc. Jpn.* **86**, 063707 (2017).
- [71] G. Baym and P. Kadanoff, *Phys. Rev.* **124**, 287 (1961).
- [72] T. Saito, Y. Yamakawa, S. Onari, and H. Kontani, *Phys. Rev. B* **92**, 134522 (2015).
- [73] R. Tazai, Y. Yamakawa, M. Tsuchiizu, and H. Kontani, *Phys. Rev. B* **94**, 115155 (2016).
- [74] R. Tazai, Y. Yamakawa, M. Tsuchiizu, and H. Kontani, *J. Phys. Soc. Jpn.* **86**, 073703 (2017).
- [75] R. Tazai and H. Kontani, *Phys. Rev. B* **98**, 205107 (2018).
- [76] N. Fujiwara, N. Kawaguchi, S. Iimura, S. Matsuishi, and H. Hosono, *Phys. Rev. B* **96**, 140507(R) (2017).
- [77] L. Fanfarillo, A. Valli, and M. Capone *Phys. Rev. Lett.* **125**, 177001 (2020).

[Supplementary Material]
**Doping effects on electronic states in electron-doped FeSe:
 Impact of self-energy and vertex corrections**

Youichi Yamakawa, Seiichiro Onari, and Hiroshi Kontani
Department of Physics, Nagoya University, Nagoya 464-8602, Japan

A. TIGHT-BINDING MODELS

We explain how we constructed the VCA tight-binding model. First, we perform the band calculation of $\text{Li}_{1-x}\text{Fe}_x\text{OHFeSe}$ using WIEN2k. Here, we employ the crystal structure of $\text{Li}_{0.8}\text{Fe}_{0.2}\text{OHFeSe}$ [1], and the doping effect is incorporated using the VCA with virtual atoms having a nuclear charge of $3+x$ being substituted for the Li sites. Next, we construct the eight-orbital d - p tight-binding model by using the Wannier90 and wien2wannier packages for $x = 0$ and $x = 0.2$; other models are obtained via interpolation.

In many Fe-based superconductors, the results of band calculations differ from the experimental results, especially for FeSe compounds [2–5]. Therefore, to reproduce the experimental Fermi surfaces (FSs), we shift the E_{xz} level at $\mathbf{k} = [(0, 0), (\pi, 0), (0, \pi), (\pi, \pi)]$ by $[-0.24, 0, +0.18, 0]$ and E_{xy} level at $\mathbf{k} = [(0, 0), (\pi/2, 0), (\pi, 0), (0, \pi/2), (\pi/2, \pi/2), (0, \pi), (\pi/2, \pi), (\pi, \pi)]$ by $[0, -0.24, +0.4, -0.24, 0, 0, +0.4, 0, -0.3]$ in unit eV, by introducing the additional inter-orbital hopping integrals for $l = xz, yz,$ and xy [6]. In addition, we enlarge the hopping parameters between d_{xy} and p_z by 1.25 times to maintain the absence of an eFS at the Γ point for $x < 0.15$. The present \mathbf{k} - and orbital-dependent shift gives $\hat{\Sigma}_{\text{exp}}$ in the main text.

Figure S1 shows the folded band dispersions for $x = 0.15$ with the spin-orbit interaction (SOI) $\eta_{\text{SOI}}\mathbf{l} \cdot \mathbf{s}$ and $\eta_{\text{SOI}} = 50$ meV. In comparison with the rigid-band (RB) model, the bandwidth obtained using the VCA decreases with doping, similarly to a previous study on K-dosed FeSe [7].

The density of states is shown in Fig. 2(c) in the main text, and there is a kink structure at $x \sim 0.25$. This kink originates from the emergence of a new electron-pocket around Γ point with e -doping. In Fig. S1, we see that the bottom of the electron-like band around Γ point is about $+0.25$ eV above the Fermi level for $x = 0.15$, whereas it touches the Fermi level for $x \sim 0.25$. The emergence of this new electron-pocket (= Lifshitz transition) has been reported in heavily e -doped compounds by ARPES studies [8, 9]. Interestingly, T_c increases by $\sim 20\text{K}$ at the Lifshitz transition [8]. It is an important future issue to understand the origin of the increment in T_c .

To estimate the value of η_{SOI} , we make a comparison between the WIEN2k band structure with spin-orbital interaction and the present tight-binding model band structure with $\eta_{\text{SOI}}\mathbf{l} \cdot \mathbf{s}$. The obtained value is $\eta_{\text{SOI}} = 52 \pm 2$ meV, which is very consistent with $\eta_{\text{SOI}} = 50$ meV

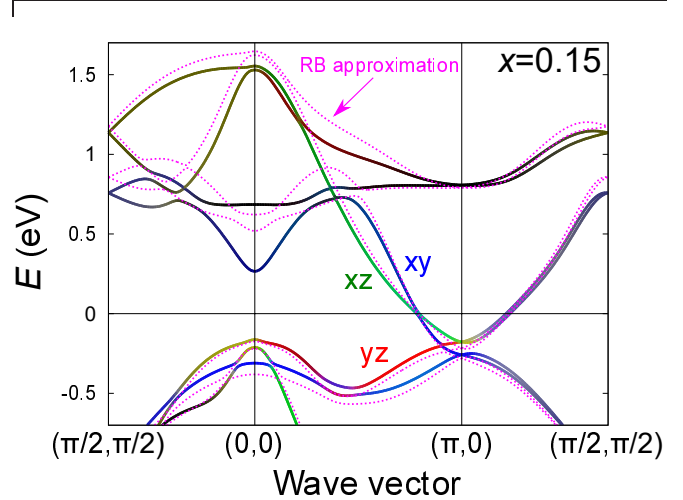


FIG. S1. Folded band dispersions for $x = 0.15$ with $\eta_{\text{SOI}} = 50$ meV. The green, red, and blue lines correspond to the xz , yz , and xy orbitals, respectively. The dotted lines represent the band dispersions in the RB model.

used in the present paper.

B. VERTEX CORRECTIONS

Here, we present the analytic expressions for the vertex corrections (VCs) used in the main text. In the SC-VC theory, the charge susceptibility is given by $\hat{\chi}^c(q) = \hat{\Phi}^c(q) [\hat{1} - \hat{U}^c \hat{\Phi}^c(q)]^{-1}$, where \hat{U}^c is the charge-channel Coulomb interaction, $\hat{\Phi}^c(q) \equiv \hat{\chi}^0(q) + \hat{X}^c(q)$ is the charge-channel irreducible susceptibility, and $\chi_{l,l';m,m'}^0 = -\frac{T}{N} \sum_k G_{l,m}(k+q) G_{m',l'}(k)$ is the bare susceptibility. The charge-channel Aslamazov-Larkin (AL)-VC, X^c , is given by [10]

$$\begin{aligned} X_{l,l';m,m'}^c(q) &= \frac{T}{N} \sum_p \sum_{\substack{l_1 \sim l_4, \\ m_1 \sim m_4}} C_{l,l_3;l_2,l'}^{l_1,l_4}(q,p) C_{m_1,m_2;m_3,m_4}^{m,m'}(q,p) \\ &\times \sum_{\nu=s,c} b_\nu \hat{V}_{l_1,l_2;m_1,m_2}^\nu(p+q) \hat{V}_{l_3,l_4;m_3,m_4}^\nu(-p), \quad (\text{S1}) \end{aligned}$$

where $b_s = \frac{3}{2}$ and $b_c = \frac{1}{2}$. The three-boson coupling \hat{C} in Fig. 1(a) is given by

$$C_{m_1,m_2;m_3,m_4}^{m,m'}(q,p) = -\frac{T}{N} \sum_{k'} G_{m',m_4}^0(k')$$

$$\times G_{m_3, m_2}^0(k' - p)G_{m_1, m}^0(k' + q), \quad (\text{S2})$$

and \hat{C}' is defined as

$$C_{m_1, m_2; m_3, m_4}^{m, m'}(q, p) \equiv C_{m_1, m_2; m_3, m_4}^{m, m'}(q, p) + C_{m_1, m_3; m_2, m_4}^{m, m'}(q, -p - q). \quad (\text{S3})$$

Next, we present the formulations of the U -VC. The U -VC is given as [11–15]

$$\hat{\Lambda}^{c(s)}(k, k') = \hat{1} + \hat{\Lambda}^{\text{MT}, c(s)}(k, k') + \hat{\Lambda}^{\text{AL}, c(s)}(k, k') \quad (\text{S4})$$

where $\hat{\Lambda}^{\text{MT}, c(s)}$ is the Maki-Thompson (MT) term, and $\hat{\Lambda}^{\text{AL}, c(s)}$ is the Aslamazov-Larkin (AL) term, both of which were introduced in Refs. [11, 12, 14]. The charge-channel AL-term is given as

$$\begin{aligned} \Lambda_{l, l'; m, m'}^{\text{AL}, c}(k, k') &= \frac{T}{N} \sum_p \sum_{m_1 \sim m_6} G_{m_1, m_2}^0(k' - p) C_{m_3, m_4; m_5, m_6}^{m, m'}(k - k', p) \\ &\times \sum_{\nu=s, c} V_{l, m_1; m_3, m_4}^\nu(k - k' + p) V_{m_2, l'; m_5, m_6}^\nu(-p). \quad (\text{S5}) \end{aligned}$$

Here, $\Lambda^{\text{AL}, c}$ and X^c have the following relation,

$$\begin{aligned} X_{l, l'; m, m'}^c(q) &= -\frac{T}{N} \sum_p \sum_{m_1, m_2} \Lambda_{l, l'; m_1, m_2}^{\text{AL}, c}(p + q, p) \\ &\times G_{m, m_1}^0(p + q) G_{m_2, m'}^0(p). \quad (\text{S6}) \end{aligned}$$

In Refs. [13–15], we verified that Λ^c is important only for low energy region near the Fermi momentum, and therefore it is important for the pairing interaction. We also verified in Ref. [14] that $\Lambda^c \sim O(1)$ if the local approximation is applied.

Finally, we introduce the crossing-fluctuation-exchange term $\hat{V}_{\text{cross}}^{\text{SC}}$ [12]. Its analytic expression is given by

$$\begin{aligned} \hat{V}_{\text{cross}}^{\text{SC}}(k, k') &= \frac{T}{4N} \sum_q \hat{G}^0(k' - q) \hat{G}^0(-k - q) \\ &\times \sum_{\nu, \nu'=c, s} b'_{\nu, \nu'} \hat{V}^\nu(k - k' + q) \hat{V}^{\nu'}(-q), \quad (\text{S7}) \end{aligned}$$

where $b'_{c, c} = -1$ and $b'_{s, s} = b'_{c, s} = b'_{s, c} = 3$.

C. NON-MAGNETIC NEMATIC STATE IN BULK AND LOW-DOPED FESE

Here, we explain the reason why the orbital order without magnetism can be realized for $x < x_c$ as shown in Fig. 4 in the main text. We concentrated on this important issue in Refs. [6, 16], and found that the relations $T_S > 0$ (positive nematic transition temperature) and $T_N < 0$ (absence of magnetism) can be satisfied in the present spin-fluctuation-driven orbital order theory.

Based on the SC-VC theory, when $\chi^s(\mathbf{Q}) \sim 1/(T - T_N)$, the predicted orbital susceptibility is $\chi^{\text{orb}}(\mathbf{0}) \sim 1/[1 - C(T)^2 T \chi^s(\mathbf{Q})]$, where $C(T)$ is the three-boson coupling in Fig. 1(a). Since $C(T)^2 \sim 1/T$ [6], then $C(T)^2 T \equiv g$ is roughly T -independent. Then, $\chi^{\text{orb}}(\mathbf{0}) \sim (T - T_N)/(T - T_S)$ with $T_S \sim T_N + g$. Therefore, $\chi^{\text{orb}}(\mathbf{0})$ diverges at a finite temperature even if $T_N < 0$ once $g > -T_N$. (We stress that, if $C(T)$ is constant, T_S is always negative if $T_N < 0$.) In addition, T_S is enlarged by the finite electron-phonon coupling.

This is supported by the DW equation analysis in Ref. [16]: As shown in Fig. 2 (d) of Ref. [16], spin Stoner factor α_S saturates as a function of r ($\propto U$) for $r > r_c = 0.257$ at a fixed temperature. The origin of the saturation is the poor-nesting caused by the sign-reversing orbital order that is obtained by the DW equation [16]. The sign-reversing orbital order is actually observed by ARPES studies [5].

To summarize, because of the (i) T -dependence of the three-boson coupling $C(T)$ and (ii) the poor-nesting caused by the sign-reversing orbital order, the relations $T_S > 0$ and $T_N < 0$ can be satisfied in the present theory.

D. DW EQUATION IN CONSERVING APPROXIMATION

Here, we discuss the charge (orbital) order based on the density-wave (DW) equation [16–19], where the form factor $\hat{f}^q(\mathbf{k})$ is taken into account. In order to satisfy the conserving approximation (CA) formalism of Baym and Kadanoff [20], we solve the following DW equation including the FLEX self-energy [21]. This CA is important to avoid unphysical results.

The DW equation is given as

$$\begin{aligned} \lambda_{\mathbf{q}} f_{l, l'}^{\mathbf{q}}(k) &= \frac{T}{N} \sum_{k'} \sum_{m_1 \sim m_4} I_{l, l'; m_1, m_2}^{c, \mathbf{q}}(k, k') \\ &\times G_{m_1, m_3}(k + q) G_{m_4, m_2}(k) f_{m_3, m_4}^{\mathbf{q}}(k'), \quad (\text{S8}) \end{aligned}$$

where $\lambda_{\mathbf{q}}$ is the eigenvalue and l, m are orbital indices.

The diagrammatic expression of the irreducible vertex \hat{I} is shown in Fig. S2(a). By solving the DW equation, the effective interaction \hat{V} shown in Fig. S2(b), which include the infinite series of \hat{I} , is generated.

Figure S2(c) shows the \mathbf{q} dependence of the $\lambda_{\mathbf{q}}$ for $x = 0$ with $r = 0.355$ and $T = 20$ meV. There is a sharp peak at $\mathbf{q} = \mathbf{0}$ [16]. The \mathbf{q} dependence of $\lambda_{\mathbf{q}}$ is consistent with the result for $\Sigma = 0$ in Refs. [16–18]. We find that the condition $\lambda \sim O(1)$ can be realized even when the self energy is included.

$\lambda_{\mathbf{q}}$ for $x = 0.25$ is shown in Fig. S2(d). In this case, the peak at $\mathbf{q} \approx \mathbf{0}$ becomes broad, and $\lambda_{\mathbf{q}}$ is large for $|\mathbf{Q}| \sim \pi/2$, which corresponds to the diameter of each electron FS. In addition, $\lambda_{\mathbf{q}}$ also develops at the inter-FS nesting vector $\mathbf{Q}' \approx (\pi, \pi/2)$. Antiferro-bond fluctuations with $\mathbf{q} \neq \mathbf{0}$ are expected to be developed in other Fe-based superconductors [18].

Here, we make a comparison between the results of DW equation and SC-VC theory. The peaks at $\mathbf{q} \sim \mathbf{0}$ for $x = 0$ and $x = 0.25$ are consistent with the ferro orbital fluctuations of SC-VC theory. On the other hand, the peak at $\mathbf{q} \sim \mathbf{Q}'$ for $x = 0.25$, which does not exist in the SC-VC theory, is the bond fluctuation, in which \mathbf{k} dependence of $f_q^{\text{DW}}(\mathbf{k})$ is essential. We will discuss it in SM. E in detail.

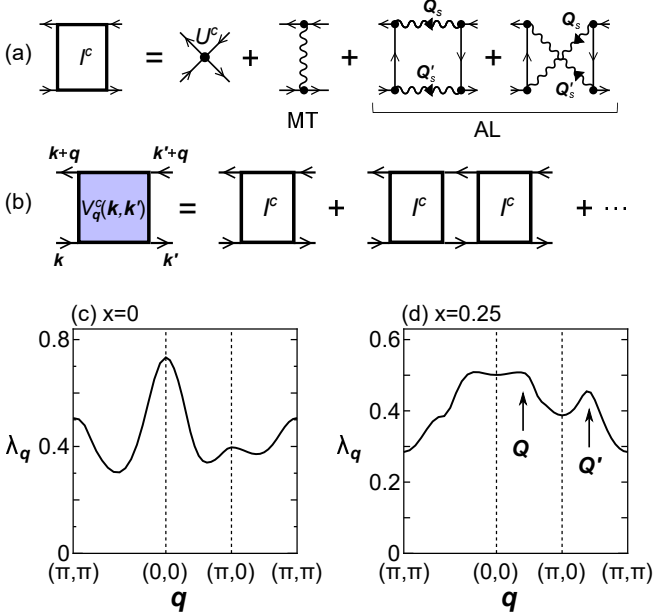


FIG. S2. (a) Charge channel irreducible kernel I^c composed of U^c , MT term, and AL terms. (b) Full four-point vertex. Momentum dependences of λ_q for (c) $x = 0$ and (d) $x = 0.25$.

E. THE CROSS TERM $V_{\text{cross}}^{\text{SC}}$: BOND FLUCTUATION CONTRIBUTION

To understand the two pairing interactions in Fig. 5(a) in a unified way, we construct the charge-channel effective interaction $V_q^c(k, k')$ composed of the irreducible kernel function $I_q^c(k, k')$ shown in Fig. S2(a). Below, we neglect the orbital indices to simplify the equation, the Bethe-Salpeter equation for $V_q^c(k, k')$ is

$$V_q^c(k, k') = I_q^c(k, k') + \frac{T}{N} \sum_p V_q^c(k, p) G(p+q) G(p) I_q^c(p, k') \quad (\text{S9})$$

Its diagrammatic expression is shown in Fig. S2 (b). Here, the kernel is well approximated as $I_q^c(k, k') \approx g f_q(k) f_q^*(k')$, where $f_q(k)$ is the form factor of the DW equation. Then, the effective interaction $V_q^c(k, k')$ is expressed as

$$V_q^c(k, k') \approx g \frac{f_q(k) f_q^*(k')}{1 - \lambda_q}, \quad (\text{S10})$$

which takes huge value when $1 - \lambda_q \lesssim 1$.

Here, we divide V_q^c into $V_q^{c(1)}$ and $V_q^{c(2)}$: The former is the set of the reducible diagrams with respect to U^c in Fig. S3(a), and the latter is the set of irreducible diagrams in Fig. S3(b). First, we examine the single pairing interaction given by $V_q^{c(1)}$; $V^{\text{SC}(1)}(k, k') \equiv V_{k-k'}^{c(1)}(k, -k')$. It corresponds to the first term in Fig. 5(a), $V_{\Lambda}^{\text{SC}}(k, k')$, if Λ^c in Fig. S3(a) is given as Fig. 5(b). Thus, $V^{\text{SC}(1)}(k, k')$ represents the orbital-fluctuation-mediated pairing interaction dressed by two U -VCs.

If the form factor has sign reversal and $\frac{1}{N} \sum_{\mathbf{k}} f_q(\mathbf{k}) \approx 0$ is satisfied, the relation $V_q^{c(2)} \gg V_q^{c(1)}$ is realized. In this case, the pairing interaction $V^{\text{SC}(2)}(k, k') \equiv V_{k-k'}^{c(2)}(k, -k')$ becomes significant. Its lowest term corresponds to the second term in Fig 5 (b), $V_{\text{cross}}^{\text{SC}}(k, k')$, which gives the large attractive inter-pocket interaction for $x = 0.20$. The Fourier transformation of $f_q(k)$ gives the bond-order, which is the modulation of hopping integrals. Thus, $V^{\text{SC}(2)}(k, k')$ represents the bond-fluctuation-mediated pairing interaction.

According to the DW equation analysis for the e-doped FeSe model in Fig. S2, strong ferro-fluctuations emerge for both $x = 0$ and $x = 0.25$, consistently with the ferro-orbital fluctuations in Figs. 4(a) and 4(b). In addition, strong incommensurate fluctuations at $\mathbf{q} \approx (\pi, \pi/2)$ develop at $x = 0.25$. They are overlooked in the SC-VC theory since the strong \mathbf{k} -dependence of the form factor is essential. This incommensurate ‘‘bond fluctuations’’ (= fluctuation of hopping integrals) is important for the pairing mechanism in heavily e-doped FeSe, as we see in Fig. 5(d).

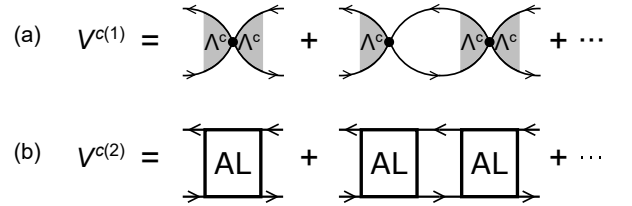


FIG. S3. (a) $V^{c(1)}$: the set of the reducible diagrams with respect to U^c in V . (b) $V^{c(2)}$: the set of irreducible diagrams.

F. SUPERCONDUCTIVITY IN BULK AND LOW-DOPED FESE

Here, we briefly discuss the superconductivity for $x \leq x_c$. For $x < x_c$, both the spin fluctuation-mediated s_{\pm} -wave state [22] and orbital fluctuation s_{++} -wave state [23] have been proposed. In both mechanisms, the orbital selective gap function in FeSe ($\Delta_{yz} \gg \Delta_{xz}, \Delta_{xy}$) [24] is reproduced well by considering the momentum dependent orbital polarization revealed by Refs. [5, 16]. With increasing x , the s_{++} -wave gap at $x = 0$ can smoothly change to the plain s-wave gap shown in Fig. 5(d). On

the other hand, the s_{\pm} -wave gap at $x = 0$ may change to the “incipient s_{\pm} -wave state” by assigning the SC gap

on the incipient hole-band below the Fermi level [25–27]. It is our important future issue to understand the experimental smooth crossover of the SC state around $x \sim x_c$.

-
- [1] X. F. Lu, N. Z. Wang, H. Wu, Y. P. Wu, D. Zhao, X. Z. Zeng, X. G. Luo, T. Wu, W. Bao, G. H. Zhang, F. Q. Huang, Q. Z. Huang, and X. H. Chen, *Nat. Mater.* **14**, 325 (2015).
- [2] J. Maletz, V. B. Zabolotnyy, D. V. Evtushinsky, S. Thirupathiah, A. U. B. Wolter, L. Harnagea, A. N. Yaresko, A. N. Vasiliev, D. A. Chareev, A. E. Böhmer, F. Hardy, T. Wolf, C. Meingast, E. D. L. Rienks, B. Buchner, and S. V. Borisenko, *Phys. Rev. B* **89**, 220506(R) (2014).
- [3] K. Nakayama, Y. Miyata, G. N. Phan, T. Sato, Y. Tanabe, T. Urata, K. Tanigaki, and T. Takahashi, *Phys. Rev. Lett.* **113**, 237001 (2014).
- [4] T. Shimojima, Y. Suzuki, T. Sonobe, A. Nakamura, M. Sakano, J. Omachi, K. Yoshioka, M. Kuwata-Gonokami, K. Ono, H. Kumigashira, A. E. Böhmer, F. Hardy, T. Wolf, C. Meingast, H. v. Löhneysen, H. Ikeda, and K. Ishizaka, *Phys. Rev. B* **90**, 121111(R) (2014).
- [5] Y. Suzuki, T. Shimojima, T. Sonobe, A. Nakamura, M. Sakano, H. Tsuji, J. Omachi, K. Yoshioka, M. Kuwata-Gonokami, T. Watashige, R. Kobayashi, S. Kasahara, T. Shibauchi, Y. Matsuda, Y. Yamakawa, H. Kontani, and K. Ishizaka, *Phys. Rev. B* **92**, 205117 (2015).
- [6] Y. Yamakawa, S. Onari, and H. Kontani, *Phys. Rev. X* **6**, 021032 (2016).
- [7] Y. W. Choi and H. J. Choi, *Phys. Rev. Lett.* **122**, 046401 (2019).
- [8] X. Shi, Z.-Q. Han, X.-L. Peng, P. Richard, T. Qian, X.-X. Wu, M.-W. Qiu, S. C. Wang, J. P. Hu, Y.-J. Sun, and H. Ding, *Nat. Commun.* **8**, 14988 (2017).
- [9] M. Ren, Y. Yan, X. Niu, R. Tao, D. Hu, R. Peng, B. Xie, J. Zhao, T. Zhang, and D.-L. Feng, *Sci. Adv.* **3**, e1603238 (2017).
- [10] S. Onari and H. Kontani, *Phys. Rev. Lett.* **109**, 137001 (2012).
- [11] S. Onari, Y. Yamakawa, and H. Kontani, *Phys. Rev. Lett.* **112**, 187001 (2014).
- [12] Y. Yamakawa and H. Kontani, *Phys. Rev. B* **96**, 045130 (2017).
- [13] R. Tazai, Y. Yamakawa, M. Tsuchiizu, and H. Kontani, *Phys. Rev. B* **94**, 115155 (2016).
- [14] R. Tazai, Y. Yamakawa, M. Tsuchiizu, and H. Kontani, *J. Phys. Soc. Jpn.* **86**, 073703 (2017).
- [15] R. Tazai and H. Kontani, *Phys. Rev. B* **98**, 205107 (2018).
- [16] S. Onari, Y. Yamakawa, and H. Kontani, *Phys. Rev. Lett.* **116**, 227001 (2016).
- [17] S. Onari and H. Kontani, *Phys. Rev. B* **100**, 020507 (2019).
- [18] S. Onari and H. Kontani, arXiv:1911.10689.
- [19] K. Kawaguchi, M. Tsuchiizu, Y. Yamakawa, and H. Kontani, *J. Phys. Soc. Jpn.* **86**, 063707 (2017).
- [20] G. Baym and P. Kadanoff, *Phys. Rev.* **124**, 287 (1961).
- [21] N. E. Bickers and S. R. White, *Phys. Rev. B* **43**, 8044 (1991).
- [22] A. Kreisel, B. M. Andersen, P. O. Sprau, A. Kostin, J. C. S. Davis, and P. J. Hirschfeld, *Phys. Rev. B* **95**, 174504 (2017).
- [23] Y. Yamakawa and H. Kontani, *Phys. Rev. B* **96**, 144509 (2017).
- [24] P. O. Sprau, A. Kostin, A. Kreisel, A. E. Böhmer, V. Taufour, P. C. Canfield, S. Mukherjee, P. J. Hirschfeld, B. M. Andersen, and J. C. S. Davis, *Science* **357**, 75 (2017).
- [25] T. Saito, S. Onari, and H. Kontani, *Phys. Rev. B* **83**, 140512(R) (2011).
- [26] X. Chen, S. Maiti, A. Linscheid, and P. J. Hirschfeld, *Phys. Rev. B* **92**, 224514 (2015).
- [27] V. Mishra, D. J. Scalapino, and T. A. Maier, *Sci. Rep.* **6**, 32078 (2016).